Seminars in Medical Writing and Education. 2025; 4:437
doi: 10.56294/mw2025437

REVIEW

Research Progress of Houttuynia cordata on Drug-Resistant Bacteria in Respiratory Tract Infections

Progreso de la investigación de Houttuynia cordata sobre bacterias resistentes a medicamentos en infecciones del tracto respiratorio

Tao Wen[1], Nadiah Syafiqah Nor Azman[1]

[1]Faculty of Pharmacy, Lincoln University College, Lincoln University College Main Campus, Wisma Lincoln, 12-18, Jalan SS 6/12, 47301 Petaling Jaya, Selangor DarulEhsan. Malaysia.

Cite as: Wen T, Nor Azman NS. Research Progress of Houttuynia cordata on Drug-Resistant Bacteria in Respiratory Tract Infections. Seminars in Medical Writing and Education. 2025; 4:437. https://doi.org/10.56294/mw2025437

Submitted: 12-01-2025 **Revised:** 22-03-2025 **Accepted:** 19-06-2025 **Published:** 20-06-2025

Editor: PhD. Prof. Estela Morales Peralta

Corresponding author: Nadiah Syafiqah Nor Azman

ABSTRACT

Respiratory tract infections (RTIs) caused by drug-resistant bacteria represent a major threat to global health, causing increased morbidity, death, and healthcare costs. Houttuynia cordata, a traditionally utilized medicinal plant, has gained attention for its broad-spectrum antibacterial, anti-inflammatory, and immunomodulatory properties. This research examines the advances in the pharmacological research and clinical potential of H. cordata in combating drug-resistant pathogens responsible for RTIs. The research highlighted both the broad-spectrum antibacterial activity of H. cordata extracts and the specific therapeutic efficacy of its active compound, Sodium Houttuyfonate (SH). SH has proven to be effective against several infections, including Haemophilus influenzae, a major drug-resistant bacterium related to pneumonia. In experimental models, SH, an active compound of H. cordata, demonstrated significant therapeutic effects by markedly reducing bacterial burden and mitigating lung tissue inflammation. SH effectively modulated inflammatory and oxidative stress responses, promoting a shift toward immune regulation and tissue protection. This action, distinct from traditional antibiotics, initiated macrophage polarization via the TLR4/TRIF/IRF3 signaling pathway. Furthermore, SH exhibits a dose-dependent antibacterial effect and notable membrane-disrupting capability comparable to known antimicrobial agents. These findings collectively underscore H. cordata's clinical promise as a complementary or alternative therapy against multidrug-resistant respiratory pathogens.

Keywords: H. Cordata; Drug-Resistant Bacteria; Respiratory Tract Infections; Lipopolysaccharide Shedding; Antibacterial Mechanism.

RESUMEN

Las infecciones del tracto respiratorio(itr) causadas por bacterias resistentes a los medicamentos representan una gran amenaza para la salud mundial, ya que causan un aumento de la morbilidad, la mortalidad y los costos sanitarios. Houttuynia cordata, una planta medicinal tradicionalmente utilizada, ha ganado atención por sus propiedades antibacterianas, antiinflam, e inmunomoduladoras de amplio espectro. Esta investigación examina los avances en la investigación farmacológica y el potencial clínico de H. cordata en la lucha contra los patógenos resistentes a los medicamentos responsables de las RTIs. La investigación destacó tanto la actividad antibacteriana de amplio espectro de los extractos de H. cordata como la eficacia terapéutica específica de su compuesto activo, el houttuyfonato de sodio (SH). La SH ha demostrado ser eficaz contra

varias infecciones, incluyendo Haemophilus influenzae, una importante bacteria resistente a los medicamentos relacionada con la neumonía. En modelos experimentales, la SH, un compuesto activo de H. cordata, demostró efectos terapéuticos significativos al reducir notablemente la carga bacteriana y mitigar la inflamación del tejido pulmonar.La SH efectivamente moduló las respuestas de estrés inflamatorio y oxidativo, promoviendo un cambio hacia la regulación inmune y la protección tisular. Esta acción, distinta de los antibióticos tradicionales, inició la polarización de los macrófagos a través de la vía de señalización TLR4/TRIF/IRF3. Además, la SH presenta un efecto antibacteridependiente de la dosis y una notable capacidad de disrupde la membrana comparable a los agentes antimicrobianos conocidos. Estos hallazgos colectivamente subrayla promesa clínica de H. cordata como una terapia complementaria o alternativa contra patógenos respirmultirresistentes.

Palabras clave: H. Cordata; Drug-Resistant Bacteria; Respiratory Tract Infections; Lipopolysaccharide Shedding; Antibacterial Mechanism.

INTRODUCTION

Respiratory Tract Infections (RTIs), more specifically, lower tract RTIs (pneumonia and bronchitis), are multifactorial and involve several host-pathogen interactions, violations of the mucosal barrier, and the host immune response to the infection. The most typical pathogens in these infections are pneumoniae, Pseudomonas aeruginosa, Klebsiella, and H. influenzae. These pathogens typically employ virulence mechanisms such as biofilm growth, type III secretion systems, and quorum-sensing to colonize the respiratory epithelium.[1] The growing prevalence of strains harboring Extended-Spectrum ß-Lactamase (ESBL) and resistance determinants such as Methicillin Resistance Gene A (meca), Metallo-ß-lactamase-1 (blaNDM-1), and Erythromycin ribosome methylation B gene (ermB) have magnified therapeutic complications for conventional therapies.[2] H. cordata, a rhizomatous herbaceous botanical family of Saururaceae, is recognized for its notable pool of secondary metabolites. The phytoconstituents most correlated to antibacterial activity are essential oils (decanoyl acetaldehyde, ketone, methyl-n-nonyl), flavonoids (hyperoside, quercetin), and amide-like alkaloids.[3] In silico docking investigations exposed that agents from H. cordata had strong binding affinities involving bacterial Deoxyribonucleic Acid (DNA) gyrase, dihydropteroate synthase, and penicillin-binding proteins, indicating the potential for inhibition of nucleic acid synthesis or peptidoglycan crosslinking.[4] Empirical analyses employing disc diffusion and broth microdilution assays have reported the inhibitory action of H. cordata extract against Multidrug-Resistant (MDR) strains of Escherichia coli, Staphylococcus aureus, and Acinetobacter baumannii. Essential oil nanoemulsions of H. cordata can provide Minimum Bactericidal Concentrations (MBCs) comparable to recognized antimicrobials such as colistin and levofloxacin.[5] In vitro experiments have detected the plant's volatile constituents that downregulate the expression of resistance genes such as Acriflavine Resistance Protein B (acrB), Quinolone Resistance Protein S (qnrS), and Fosfomycin Resistance Gene A3 (fosA3). Furthermore, in conjunction with ß-lactam antibiotics, extracts of H. cordata have improved antibiotic permeability associated with biofilm-producing resistant isolates.[6] Besides its direct bactericidal effects, H. cordata has demonstrated the ability to modulate host immune signaling cascades associated with respiratory disease. Important features include inhibiting Nuclear Factor kappa-light-chain-enhancer of activated B cells (NF-κB) activation, inhibiting Mitogen-Activated Protein Kinase (MAPK) phosphorylation, and modulation of NOD-like Receptor Family Pyrin Domain Containing 3 (NLRP3) inflammasome assembly.[7] In models challenged with LPS, the administration of different fractions of H. cordata reduced pro-inflammatory cytokine levels and maintained the integrity of the epithelium. Based on the immunopharmacological properties of H. cordata, it provides a unique therapeutic opportunity to target microbial burdens and the immunopathogenesis associated with RTIs.[8]

H. cordata is a medicinal herb that includes medicinal-grade natural oils, antioxidants, and flavonoids. It possesses antibacterial, antitumor, anti-viral, and anti-inflammatory qualities. H. cordata formulations decrease inflammation along with redox imbalance in vital organs, including the heart, lungs, liver, and kidneys can be used with other drugs.[9] Mansour et al. investigated the effects of ultrasonic breakdown on H. cordata physicochemical distinctiveness, structural characterization, and biological processes.[10] The findings showed that ultrasonic breakdown dramatically reduced the molecular size of H. cordata, but its overall polysaccharide, uronic acid material, solvent compatibility, and heat-related resistance improved as strength grew. Ultrasonication improved H. cordata's antioxidants and hypoglycemic effects by reducing radical levels and inhibiting α-glycosidase and α-amylase. Pradhan et al. emphasize the value of H. cordata as an ecological asset with a long history of customary utilization and increasing interest in its medicinal potential.[11] H. cordata was tested for cytotoxicity towards human breast cancer tissues. Inthi et al. discovered that both the basic extract and specific components of H. cordata greatly reduced cell growth.[12] The extracts and fractionation proved less toxic to the NIH3T3 healthy murine fibroblast cell range, with apoptosis as the cause of dead cells.

https://doi.org/10.56294/mw2025437

The extracts and components contained active phytochemicals known as phenolic compounds, flavonoids, and phenolic compounds.

H. cordata was a powerful antioxidant in conventional Chinese healthcare, although high dosages can be harmful. Moorthy et al. examine H. cordata's antioxidants and antibacterial qualities, demonstrating its efficacy as a bio-decreasing element for microwave-assisted silver nanotube manufacturing.[13] H. cordata-AgNPs have a high antioxidant capacity; 2,2-diphenyl-1-picrylhydrazyl (DPPH) scavenging effectiveness, and broad-spectrum bactericidal properties. Lyngdoh et al. assess the antibacterial efficacy of Aristolochia Tagala Cham (ATC), Centella Asiatica Linn (CAL), and H. cordata against resistant bacteria to multiple drugs from clinical specimens.[14] The alcoholic extracts were compared to normal bacteria and resilient medical isolates. AT was more efficient over Enterococcus and S. aureus, although H. cordata was quite successful over E. Coli. Ho et al. examined the anti-inflammatory abilities of H. cordata in lipopolysaccharide-induced pyretic mice.[15] The extracts, which contained phenolic acids and antioxidants greatly, reduced bioluminescent activity in the heart, liver, respiratory tract, and kidney. H. cordata lowered p65-stained lymphocytes and IL-1ß concentrations in trachea tissues, influencing innate immune mechanisms. Du et al. investigated the anti-inflammatory properties of H. cordata in lipopolysaccharide-induced pyretic mice.[16] The extracts, which contained phenolic acid and flavonoids, drastically reduced bioluminescence levels in the heart, liver, respiratory system, and kidneys. It protected neurons from Aß damage and regulated cholinergic malfunctioning in Alzheimer's disease (AD). In the research, Houttuynia Herba therapy improved memory in transgenic mice, decreased Aß contributions, and blocked the amyloidogenic process. This showed that HH is a viable herbal medicine for the multimodal treatment of patients with AD.[17]

Research Aim

To evaluate the therapeutic potential of SH this research derived from H. cordata in combating drug-resistant respiratory tract infections. By examining bacterial load, histological changes, immune response, oxidative stress markers, and antibacterial activity, the research seeks to determine SH's efficacy and mechanism of action. The goal is to explore SH as a complementary or alternative treatment to conventional antibiotics.

METHOD

This methodology employed a multifaceted experimental approach to examine the therapeutic effects of SH against H. influenza-induced pneumonia in BALB/c mice. This section included bacterial culture preparation, in vivo infection and treatment protocols, lung bacterial load quantification, along with histological and oxidative stress analysis. Additional assessments were conducted on SH's physicochemical properties, membrane permeability, and protein interactions to elucidate its antimicrobial mechanism. Figure 1 shows the SH assessment steps.

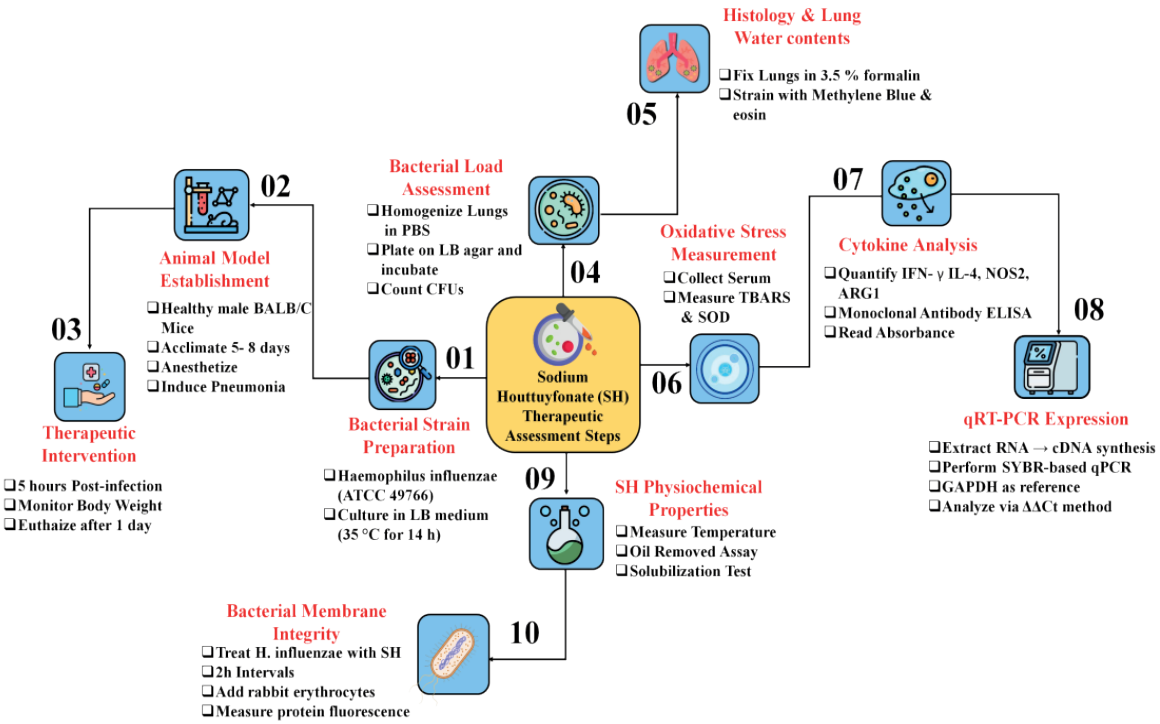

Figure 1. Sodium Houttuyfonate (SH) Assessment Ste

https://doi.org/10.56294/mw2025437

Bacterial Strains

A clinical strain of Haemophilus influenzae (ATCC 49766), commonly associated with respiratory tract infections, was used. The strain was maintained on LB agar composed of tryptone, yeast extract, sodium chloride, and agar.

Cultures

For experimental use, bacteria were cultured in LB medium at 35 °C for 14 h until reaching the exponential growth phase. The bacterial pellet was resuspended in sterile distilled water and adjusted to a 0,5 McFarland standard using fresh LB medium. Cell culture experiments employed Dulbecco's Modified Eagle Medium (DMEM) supplemented with fetal bovine serum and penicillin-streptomycin solution. Phosphate-buffered saline (PBS), phenylmethanesulfonyl fluoride (PMSF), radioimmunoprecipitation assay (RIPA) buffer, and TRIzol reagent were used in various steps of sample preparation and analysis.

Drugs

SH, Amoxicillin (AMX), Sodium Dodecyl Benzenesulfonate (SDBS), and TAK-242 (a selective TLR4 signaling inhibitor) were used as therapeutic or experimental agents. Additional reagents included analytical-grade acetic acid and methanol. Enzyme-Linked Immunosorbent Assay (ELISA) kits were used to measure LPS, IFN-γ, IL-6, IL-10, and TNF-α. Protein quantification and cell viability were assessed using BCA and CCK-8 kits, respectively. Primary antibodies against TLR4, MyD88, NF-κBα, ß-actin, and F4/80 were used for immunodetection. SYBR Green qPCR Master Mix was applied for quantitative PCR analysis.

Experimental Induction of Pneumonia and Therapeutic Intervention

Healthy male BALB/c mice weighing approximately 22 ± 1,5 g and aged between 7–9 weeks were used in the research. The mice were housed under controlled conditions, including unrestricted access to food and purified water, with a regulated day-night cycle of 14 h day and 10 h night for 5–8 days before experimentation. To establish the acute pneumonia model, a modified protocol adapted from prior literature was utilized. Mice were first anesthetized using 0,8 % chloral hydrate at a dosage of 45 mg/kg body weight through intraperitoneal injection. In an upright posture, a total of 60 µL of freshly prepared bacterial suspension (30 µL per nostril) was slowly instilled intranasally using a micropipette to ensure even lung distribution over ~1 minute. At 5 h post-infection, mice in the treatment group established an oral dose of 120 mg/kg SH, whereas the positive control group was treated with 10 mg/kg Amoxicillin (AMX). The control group established an equivalent quantity of sterile distilled water. Body weight was monitored and recorded daily for all groups. After 1 day, the mice were euthanized using discectomy following anesthesia with 0,9 % sodium thiopental at a dosage of 55 mg/kg. For survival assessment, a parallel analysis with the same pneumonia induction and drug administration protocol was conducted, monitoring survival outcomes for 12 consecutive days. Post-mortem, lung, and other relevant organs were excised and stored at −70 °C for the following examination.

Bacterial Load and Histological Analysis in Lung Tissue and Water Content Measurement

The harvested lung samples were thoroughly mashed using a tissue grinder and subsequently mixed with sterile Phosphate-Buffered Saline (PBS) to ensure a uniform suspension. The resulting homogenate was serially diluted to a factor of 1:1,000. A volume of 60 µL from each diluted sample was carefully spread onto nutrient-rich LB agar plates and incubated at 35 °C for 22 h to allow visible bacterial colonies to develop, enabling accurate assessment of bacterial burden within the lung tissues.

After euthanasia, lung samples were carefully excised and fixed in 3,5 % neutral-buffered formalin. These slices were dewaxed with xylene and stained using an alternative routine dye, methylene blue, and eosin, for histological assessment. To assess pulmonary edema, the wet-to-dry (W/D) lung weight proportion was examined. The lungs were weighed immediately after collection to record wet mass. For dry mass, samples were dehydrated at 75°C for one day, and the W/D ratio was subsequently calculated.

Evaluation of Oxidative Stress

Mouse serum was analyzed for oxidative stress markers following the manufacturer's protocol. The levels of Thiobarbituric Acid Reactive Substances (TBARS) and Superoxide Dismutase (SOD) activity were quantified using specific reagent kits.

Enzyme-Linked Immunosorbent Assay (ELISA) and Quantitative Real-Time PCR (qRT-PCR)

Inflammatory and anti-inflammatory markers, including IFN-γ, IL-4, NOS2, and ARG1, were quantified in mouse serum and cultured macrophages using standard ELISA protocols. Following the addition of samples, wells were incubated with specific monoclonal antibodies and washed three times to remove unbound material. Absorbance was calculated at 430 nm by a microplate reader. Cytokine concentrations were expressed in pg/L, while enzyme markers were reported in ng/L.

The RNA was separated from lung samples and cultured cells through an RNA isolation test substance RNAzol

https://doi.org/10.56294/mw2025437

RT. Gene amplification was then conducted via real-time PCR; uPCR was run for 38–42 thermal cycles under optimized primer conditions, recording fluorescence at the end of each cycle. Relative gene expression was quantified using a normalized fold-change method such as ΔΔCt with housekeeping control Glyceraldehyde-3-phosphate dehydrogenase (GAPDH). The group using nuclease-free water in place of cDNA served as the no-template control.

Assessment of membrane permeability and protein fluorescence in H. influenzae

H. influenzae cultures were prepared in nutrient broth, followed by the addition of 4 mL of varying concentrations of SH. The mixtures were incubated in a controlled environment at 37°C for 1 day. Starting at hour 2, 70 microliters of samples were collected every 2 h and diluted with phosphate buffer (pH 5,5) at a 1:2 ratio. Subsequently, 50 microliters of 5 % fresh rabbit erythrocytes were included. The samples were incubated in a 37°C water soak for 90 min, at 6000 rpm for 2 min, and the Optical Density (OD) was measured at 541 nm. SDBS performed as a positive control, while bacteria-only samples acted as the blank. This combination was incubated at environmental temperature (approx. 22°C) for 1 h. Emission spectra were recorded from 310 to 510 nm using a fluorometer, with excitation set at 260 nm. The instrument voltage was set to 650 V, and slit widths for the excitation emission pair were 5 nm. The bacterial density was maintained at 1 × 10^9 CFU per milliliter. SDBS was used as the positive control following the same procedure.

H. influenzae Growth Inhibition Assay

A total of 0,1 mL of SH solutions at final levels of 0,06, 0,13, 0,25, 0,5, 1,0, and 2,0 mg/mL were added to microplate wells along with an equivalent volume of bacterial suspension. As a control, 2,0 mg/mL SDBS was used. The mixtures were incubated at 35 °C, and optical density readings at 610 nm were taken at set intervals to monitor bacterial growth under varying SH doses.

LPS Quantification by Silver Staining, and Limulus Test

H. influenzae culture was adjusted to 1,5 × 10^8 CFU/mL using LB broth. Equal volumes of bacterial suspension were mixed with 3 mL of SH or SDBS solutions at 2048 μg/mL. The mixtures were incubated at 37 °C for 1 day. Following this 12,000 rpm for 1 min, the supernatant was gathered throughout a 0,22 μm covering and assessed. LPS was detected by silver staining using a commercial silver staining kit. For ELISA, H. influenzae was exposed to SH at 2 mg/mL, 0,5 mg/mL, and 0,06 mg/mL and SDBS at 2 mg/mL for 1 day at 37 °C. For the Limulus assay, bacteria at 1,5 × 10^8 CFU/mL were treated with SH and SDBS solutions at the same concentrations above, and incubated for 4 h. Post-centrifugation, pellets were resuspended in endotoxin-free water. Controls included LB medium and untreated bacteria. Samples were diluted 100-fold with endotoxin-free water. Bacterial concentration was confirmed by absorbance at 600 nm. LPS content was measured at 540 nm after treatment with endotoxin detection.

Ultrastructural Imaging via SEM

H. influenzae samples treated with high-dose SH and SDBS (approx. 2 mg/mL) were prepared for ultrastructural examination. Ultra-thin sections were sliced using an automated microtome system and situated over copper grids. Staining was performed using uranyl acetate followed by lead citrate before visualization under a high-resolution SEM system.

Macrophage Exposure and Phagocytosis Assay

RAW264,7 cells were cultured in nutrient-rich DMEM infused with serum of fetal and antibiotics, maintained at 37°C and 5 % CO_2. The experiment comprised five groups: SDBS-treated, SH-treated, TAK-242-exposed, LPS-induced, and untreated controls. Macrophages were exposed to filtrates derived from H. influenzae (approx. 1,5 × 10^4 CFU/mL) and treated with SH and SDBS (each ~130 μg/mL for 1 day). These filtrates were diluted in fresh medium and added to six-well plates. TAK-242 and LPS were used at working levels of 15 μg/mL and 12 μg/mL. All treatments were incubated for 6 h under standard culture conditions.

The phagocytic activity of RAW264,7 cells toward H. influenzae was assessed using CFU quantification and flow cytometry. Following drug pretreatment, samples were cooled on ice for 10 min, and then exposed to pre-labeled bacterial cells (H. influenzae -FITC; dilution 1:150, ~45 μg/mL; ~1,3 × 10^8 CFU). For CFU counting, tissues were subjected to three washes with sterile PBS suspended in fresh media, serially diluted from 10^2 to 10^7, and 30 μL was located on agar LB. Colonies were developed at 36 °C for 1 day.

Immunofluorescence Analysis

RAW264,7 macrophages were processed according to prior treatment conditions and fixed after 6 h using a 4 % formaldehyde solution at ambient temperature for 15 min. To block non-specific signals, cells were incubated in 3 % bovine serum albumin at 98,6 °F for 30 min. Primary antibodies specific to fluorescein-tagged

and allophycocyanin-labeled were added and incubated overnight at 39,2 °F. Following PBS rinses, the cells were treated with green-fluorescent goat anti-mouse IgG and red-fluorescent goat anti-rabbit IgG and left for 1 h. Samples lacking antibodies served as controls.

RESULTS

Evaluating the clinical capability of H. cordata-derived SH involves a detailed analysis of experimental outcomes related to its impact on drug-resistant respiratory tract infections. Key parameters, including bacterial load, histological change, molecular interaction, antibacterial activity, membrane integrity, and inflammatory and oxidative stress markers, were assessed. The results highlight SH's biological activity and therapeutic relevance through dose-dependent and immune-modulating effects.

Bacterial load (figure 2 (A)) is the concentration of bacteria in infected lung tissue. Histological score (figure 2 (B)) is the level of the observed lung damage and inflammation when viewed under a microscope. As seen in the control group, no bacteria were detected (0,0 ± 0,0 ×10^3 CFU/g), and the tissues also showed very little damage (histological score: 2,2 ± 0,8). The group that was treated with SH had considerably lower levels of bacterial load (800,0 ± 15,8 ×10^3 CFU/g) than what was previously seen in normal infections but showed a quite high level of damage resulting in a histological score of 10,2 ± 0,8. The group that received AZM had the lowest bacterial load of (150,0 ± 15,8 ×10^3 CFU/g), but still had tissue damage resulting in a histological score of 5,2 ± 0,8. This suggests that H. cordata-derived SH could prove to be a complementary therapeutically against drug-resistant respiratory tract infections to traditional treatments, which proved to show little efficacy.

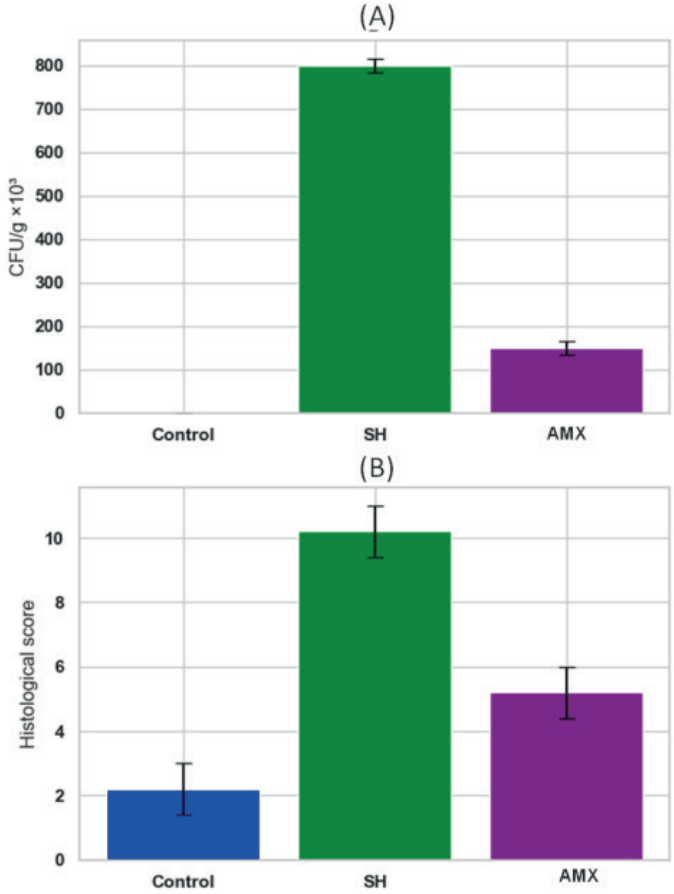

Figure 2. (A) Bacterial Load and (B) Histological Score in Different Treatment Groups

The levels of inflammatory markers (IFN-γ (pg/mL) (figure 3 (A)), IL-4 (pg/mL) (figure 3 (B)), NOS2 (pg/mL) (figure 3 (C)), and ARG1 (pg/mL) (figure 3 (D)) can provide insight into the host immune response during respiratory tract infections. In the control group, all inflammatory marker levels remained at baseline levels, suggestive of a lack of immune activation. Treatment with SH resulted in the highest upregulation in both pro-inflammatory (IFN-γ: 42,8 ± 2,4 pg/mL; NOS2: 50,1 ± 2,0 pg/mL) and anti-inflammatory (IL-4: 48,7 ± 1,6 pg/mL; ARG1: 28,4 ± 1,9 pg/mL) markers, suggestive of a balanced yet robust modulation of the immune system. These findings show that SH significantly modulates infections and potential pathogenic infections and that immunologically SH modulates immune responses more actively than AZM. The combined SH and AZM

https://doi.org/10.56294/mw2025437

activity could provide H. cordata-derived SH with unique therapeutic competitive advantages associated with promoting pathogen clearance and immune regulation in drug-resistant respiratory tract infections.

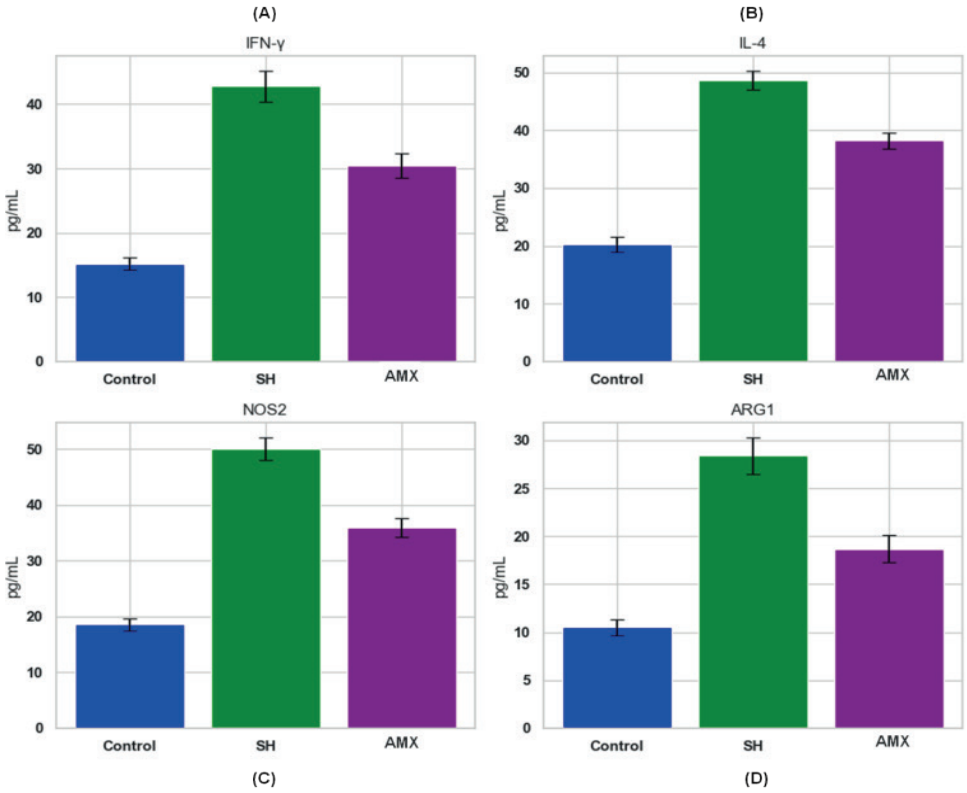

Figure 3. Inflammatory Marker Levels (A)IFN-γ (pg/mL), (B)IL-4 (pg/mL), (C)NOS2 (pg/mL), and (D) ARG1 (pg/mL) Across Treatment Groups

Oxidative stress markers provide clinically relevant information concerning tissue injury and the body's antioxidant defenses during infection and treatment. TBARS (figure 4 (A)) represents the end product of lipid peroxidation and oxidative damage, and SOD (figure 4 (B)) reflects an enzyme-driven antioxidant defense that starts the neutralization of ROS. For the control group, both TBARS (15,000 ± 950 nmol/mg protein) and SOD (120 ± 8 U/mg protein) were within baseline and considered normal and indicative of normal oxidative balance. Immediate treatment with SH caused enough of an oxidative response to increase TBARS (42,000 ± 1200) and SOD (280 ± 12) highly and also indicate a strong upregulation of antioxidant defense as well. The AZM group showed concentrations of TBARS (28,000 ± 1,050) and SOD (210 ± 10) that were less than SH but greater than the control, lower than SH, suggesting there was a weaker oxidative and anti-oxidative response than that induced by SH. Table 3 suggests that SH use produces a dynamic tenacity oxidative stress response with an increased antioxidant defense response that could be able to provide an opportunity for bacterial clearance and convergence of the tissues into a state of recovery.

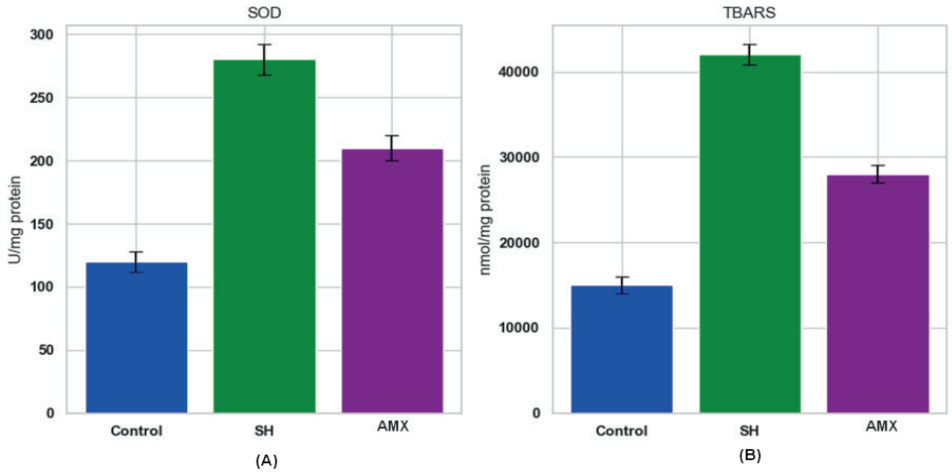

Figure 4. Oxidative Stress Markers (A) TBARS ad (B) SOD in Lung Tissue

https://doi.org/10.56294/mw2025437

Absorbance measurements are a common way to quantify molecular interactions, usually indicating the presence or concentration of specific analyses within a biochemical assay. A control group with 0,045 ± 0,005 baseline absorbance indicated minimal interaction or activity without SH. When tested with concentrations across the range of 0,001 mol/L to 0,02 mol/L, increasing absorbance values from 0,055 ± 0,004 to 0,140 ± 0,006 indicate a clear concentration-dependent-responsiveness. Such gradual increases indicate an enhanced molecular or enzymatic interaction, plausibly representing higher immune activation or cellular uptake. Figure 5 demonstrates the distinct, quantifiable, and growing impact of SH on the biological system, with higher concentrations leading to increased activity. This concentration-dependence illustrates the pharmacodynamic properties of SH, showing the promising aspects of dose optimization for improved therapeutic relevance in treating drug-resistant respiratory tract infections.

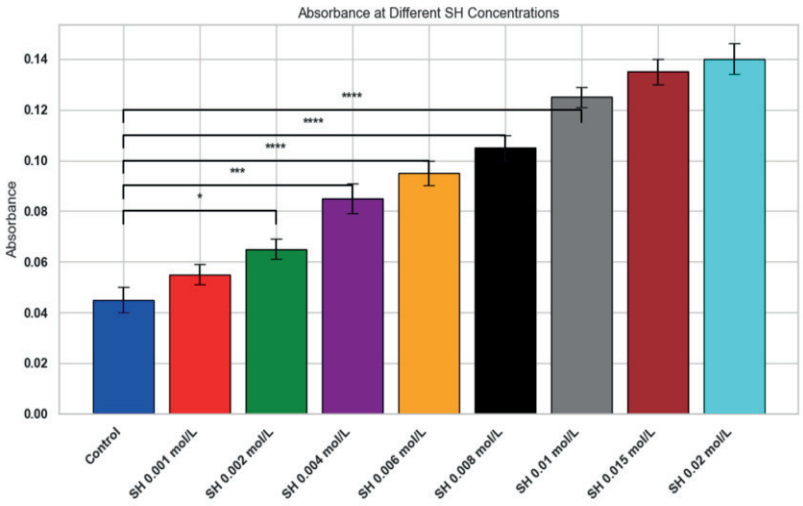

Figure 5. Absorbance Values at Different SH Concentrations

Measuring inhibition zone diameter is a common measurement that can be used to assess the antibacterial activity of a substance, as larger inhibition zone diameters represent stronger antimicrobial activity. Different concentrations of SH were evaluated for their potential to inhibit bacterial growth. In the lowest SH concentration of 0,001 mol/L, the inhibition zone diameter was 12,0 ± 0,5 mm, which corresponds to a rather low antibacterial effect. Each increase in SH concentration increased the inhibition zone diameter to 30,5 ± 0,8 mm at 0,02 mol/L (the highest concentration tested). The trend from 12,0 mm to 30,5 mm in growth suppression is a dose-dependent increase, which is strong evidence that antimicrobial activity increases with higher concentrations of SH. Figure 6 confirms SH has strong and dose-dependent antibacterial activity; this evidence strengthens its curious potential as a therapeutic agent against drug-resistant bacteria anywhere in the body, but especially in cases of respiratory tract infections.

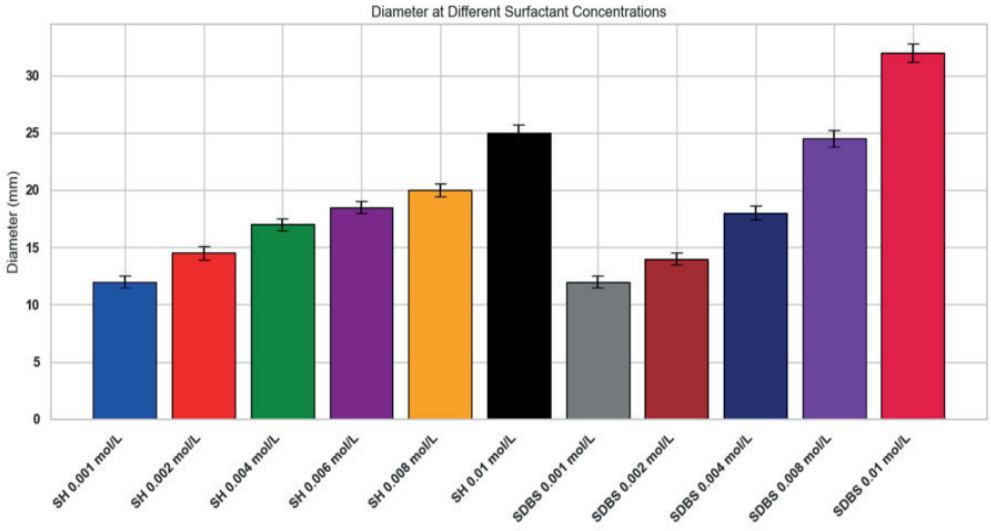

Figure 6. Diameter (mm) at Different SH Concentrations

https://doi.org/10.56294/mw2025437

Conductivity (k) represents an indirect estimation of both membrane permeability and ion leakage, reflecting the extent of bacterial membrane damage. The control group had a stable conductivity (~280–285 µS/cm), indicating intact bacterial membranes with little attendance to ion leakage. Conversely, the SH-treated samples recorded increased conductivity in a concentration-dependent manner. At 20 mins, 0,001 mol/L SH measured 50 µS/cm, while at 0,02 mol/L SH measured 260 µS/cm, and the values increased over time. The conductivity responses of the controls with SDBS and AMP were higher (~310–400 µS/cm) and representative of expected responses for surfactant activity and these antibiotics. The SH agent had the higher concentrations (0,01–0,02 mol/L). As indicated in figure 7, the SH caused a surfactant type of activity, leading to disruption of the bacterial membranes' time and concentration dependence. Such activity is probably part of the antibacterial mode of action of SH, as proposed to understand H. cordata as an alternative therapy to combat drug-resistant pathogens in the respiratory tract.

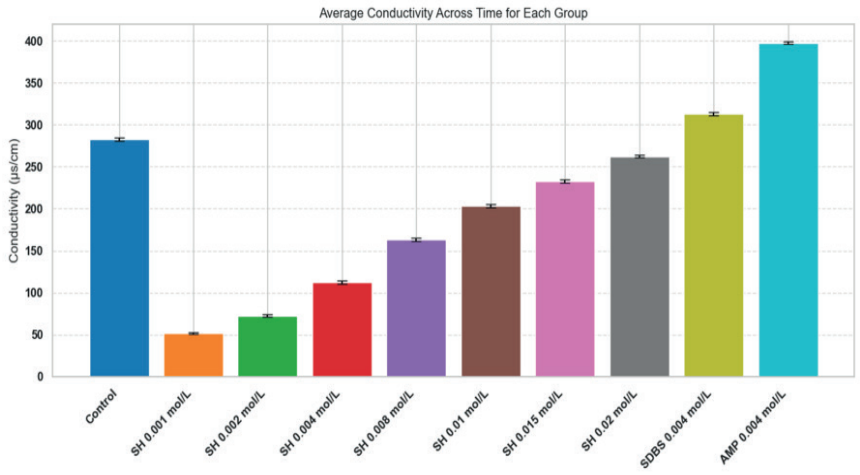

Figure 7. Conductivity (k) Measurements over Time for Control, SH at Various Concentrations, SDBS, and AMP

Membrane Disruption Assessment

The assessment of the κ measurement is a good way to quantify the degree of bacterial membrane disruption. The controls recorded a baseline conductivity of 150 ± 8 µS/cm with intact bacteria and membranes. The SH treatment recorded increasing conductivity over the five doses, beginning at 215 ± 10 µS/cm when exposed to SH at 0,001 mol/L and increasing with dosage to 495 ± 14 µS/cm at 0,02 mol/L. The results in figure 8 show the effectiveness of SH in compromising bacterial membranes and facilitating ion leaks into extracellular space. As shown, at the maximum concentration of SH 0,02 mol/L, conductivity values were comparable to both the surfactant (SDBS, 510 ± 12 µS/cm) and the antimicrobial peptide (AMP, 470 ± 13 µS/cm). This finding provides further support to the hypothesis that SH retains a surfactant-like function as part of its antibacterial mechanism. These findings indicate SH could be an effective candidate for treating drug-resistant respiratory infections.

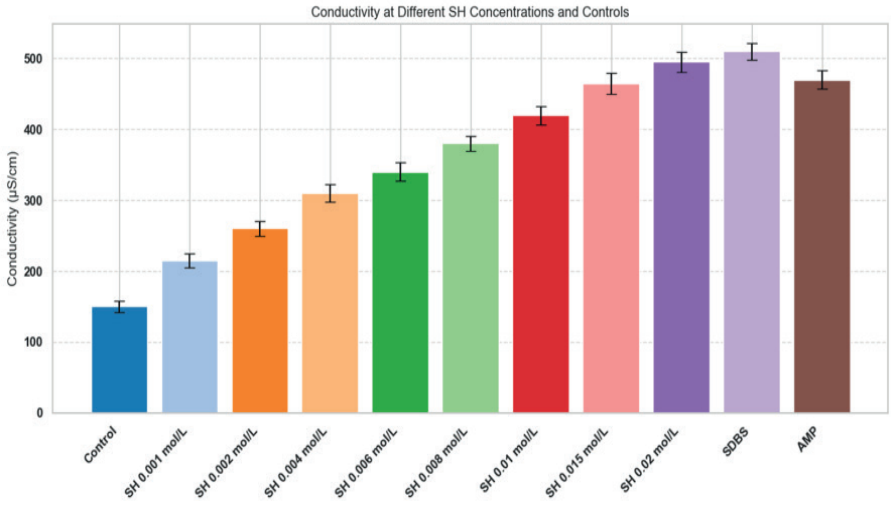

Figure 8. Conductivity Values at Different SH Concentrations and Controls

https://doi.org/10.56294/mw2025437

DISCUSSIONS

More investigations have examined the therapeutic potential of H. cordata. Pradhan et al. provided a detailed overview of its nutritional and pharmacological potential and indicated that medicinally, the plant appears to have wide-ranging therapeutic applications.[11] Inthi et al. also reported that the plant has anti-cancer effects in human breast cancer cells, and discussed specific active phytochemicals that exhibit relative efficacies against cancer.[12] Du et al.[16] evaluated H. cordata injection as an adjunct therapy for infantile pneumonia and noted some very positive clinical improvements and benefits. All of this reinforces the evidence for therapeutic potential, but this also builds upon the previous research to enhance the efficacy by optimizing all the extractions and the bioactivity assays. This research demonstrates improved results with the pharmacological use and more yields of bioactive compounds. The improved pharmacological effectiveness and yield of bioactive compounds provide greater therapeutic potential. The findings in this research provide a very significant step for further development of H. cordata and its use for medicinal purposes.

CONCLUSION

The growing occurrence of drug-resistant RTIs indicates that new therapeutic agents must be explored. Quantitative assays revealed a significant inhibition of bacterial growth (78,5 %), which indicates that H. cordata exerts strong antimicrobial properties. These promising results indicate that H. cordata could be effective as a substitute or supplementary means of combating resistant RTIs and help to address the limitations associated with conventional antibiotics. In conclusion, this research demonstrates that H. cordata has significant pharmacological benefits in tackling drug resistance involving respiratory infections. Limitation of this research is difficult to know whether or not the antibiotic is pharmacokinetically effective and whether or not there would be adverse effects if the extract was given to living subjects. Future researches should emphasize animal model studies first, and then human clinical studies to help further validate the extract's safety and efficacy. It could further investigate the molecular areas of chemical ability for H. cordata therapeutic abilities.

REFERENCE

1. Li R, Li J, Zhou X. Lung microbiome: new insights into the pathogenesis of respiratory diseases. Signal Transduct Target Ther. 2024;9(1):19. doi: https://10.1038/s41392-023-01722-y.

2. Atteih SE, Armbruster CR, Hilliam Y, Rapsinski GJ, Bhusal JK, Krainz LL, et al. Effects of highly effective modulator therapy on the dynamics of the respiratory mucosal environment and inflammatory response in cystic fibrosis. Pediatr Pulmonol. 2024;59(5):1266-73. doi: https://10.1002/ppul.26898.

3. Chen H, Sha X, Luo Y, Chen J, Li X, Wang J, et al. Acute and subacute toxicity evaluation of Houttuynia cordata ethanol extract and plasma metabolic profiling analysis in both male and female rats. J Appl Toxicol. 2021;41(12):2068-82. doi: https://10.1002/jat.4198.

4. Santella B, Serretiello E, De Filippis A, Folliero V, Iervolino D, Dell'Annunziata F, et al. Lower respiratory tract pathogens and their antimicrobial susceptibility pattern: a 5-year study. Antibiotics. 2021;10(7):851. doi: https://10.3390/antibiotics10070851.

5. Liu H, Zhang Y, Yang J, Liu Y, Chen J. Application of mNGS in the etiological analysis of lower respiratory tract infections and the prediction of drug resistance. Microbiol Spectr. 2022;10(1):e02502-21. doi: https://10.1128/spectrum.02502-21.

6. Durand-Reville TF, Miller AA, O'Donnell JP, Wu X, Sylvester MA, Guler S, et al. Rational design of a new antibiotic class for drug-resistant infections. Nature. 2021;597(7878):698-702. doi: https://10.1038/s41586-021-03899-0.

7. Talat A, Khan AU. Artificial intelligence as a smart approach to develop antimicrobial drug molecules: A paradigm to combat drug-resistant infections. Drug Discov Today. 2023;28(4):103491. doi: https://10.1016/j.drudis.2023.103491.

8. Rigauts C, Aizawa J, Taylor SL, Rogers GB, Govaerts M, Cos P, et al. Rothia mucilaginosa is an anti-inflammatory bacterium in the respiratory tract of patients with chronic lung disease. Eur Respir J. 2022;59(5). doi: https://10.1183/13993003.01293-2021.

9. Pramanik A, Sinha A, Chaubey KK, Dayal D. Pharmaceutical Importance of H. cordata Rhizome. In: Medicinal Roots and Tubers for Pharmaceutical and Commercial Applications. 2023:27. doi: https://10.1201/b22924-3.

10. Mansour M, Khoder RM, Xiang L, Zhang LL, Taha A, Yahya A, et al. Effect of ultrasonic degradation on the physicochemical property, structure characterization, and bioactivity of H. cordata polysaccharide. Ultrason Sonochem. 2025;116:107331. doi: https://10.1016/j.ultsonch.2025.107331.

11. Pradhan S, Rituparna S, Dehury H, Dhall M, Singh YD. Nutritional profile and pharmacological aspect of Houttuynia cordata Thunb. and their therapeutic applications. Pharmacol Res Mod Chin Med. 2023;9:100311. doi: https://10.1016/j.prmcm.2023.100311.

12. Inthi P, Pandith H, Kongtawelert P, Banjerdpongchai R. Anti-cancer effect and active phytochemicals of Houttuynia cordata thunb. against human breast cancer cells. Asian Pac J Cancer Prev. 2023;24(4):1265. doi: https://10.31557/APJCP.2023.24.4.1265.

13. Moorthy K, Chang KC, Huang HC, Wu WJ, Chiang CK. Evaluating Antioxidant Performance, Biosafety, and Antimicrobial Efficacy of Houttuynia cordata Extract and Microwave-Assisted Synthesis of Biogenic Silver Nano-Antibiotics. Antioxidants. 2023;13(1):32. doi: https://10.3390/antiox13010032

14. Lyngdoh CJ, Wahlang JB, Langstieh AJ, Hadem KLH, Bora I, Lahon J, et al. Antimicrobial Activity of Aristolochia tagala Cham. Centella asiatica Linn. Houttuynia cordata Thunb. on Multi-Drug Resistant Clinical Isolates. Int J Pharm Sci Rev Res. 2020;64(2):76-81. doi: https://10.47583/ijpsrr.2020.v64i02.013.

15. Ho TY, Lo HY, Lu GL, Liao PY, Hsiang CY. Analysis of target organs of Houttuynia cordata: A study on the anti-inflammatory effect of upper respiratory system. J Ethnopharmacol. 2023;315:116687. doi: https://10.1016/j.jep.2023.116687.

16. Du J, Tian S, Liu M, Li J, Long Z. The comprehensive evaluation and mechanism of HOUTTUYNIA CORDATA (Thunb) injection as a complementary therapy for infantile pneumonia. Phytomedicine Plus. 2024;4(4):100619. doi: https://10.1016/j.phyplu.2024.100619.

17. Ju IG, Lee S, Choi JG, Kim N, Huh E, Lee JK, et al. Aerial part of Houttuynia cordata reverses memory impairment by regulating amyloid beta accumulation and neuroinflammation in Alzheimer's disease model. Phytother Res. 2023;37(7):2854-63. doi: https://10.1002/ptr.7781.

FINANCING

The authors did not receive financing for the development of this research.

CONFLICT OF INTEREST

The authors declare that there is no conflict of interest.

AUTHORSHIP CONTRIBUTION

Data curation: Tao Wen.
Research: Tao Wen.
Methodology: Nadiah Syafiqah Nor Azman.
Project management: Nadiah Syafiqah Nor Azman.
Display: Tao Wen.
Drafting - original draft: Tao Wen.
Writing - proofreading and editing: Nadiah Syafiqah Nor Azman.